New determination of the $^{12}C(\alpha,\gamma)^{16}O$ reaction rate from γ-ray angular distribution measurements.

J.W. Hammer[a], M. Fey[a], R. Kunz[a], J. Kiener[b], V. Tatischeff[b], F. Haas[c], J.L. Weil[d], M. Assunção[b], C. Beck[c], C. Boukari-Pelissie[b], A. Coc[b], J.J. Correia[b], S. Courtin[c], F. Fleurot[e], E. Galanopoulos[f], C. Grama[b], F. Hammache[g], S. Harissopulos[f], A. Korichi[b], E. Krmpotić[a], D. Le Du[b], A. Lopez-Martens[b], D. Malcherek[a], R. Meunier[b], P. Papka[c], T. Paradellis[f], M. Rousseau[c], N. Rowley[c], G. Staudt[h], S. Szilner[c]

[a]Institut für Strahlenphysik (IfS), Universität Stuttgart, D-70550 Stuttgart,Germany

[b]CSNSM Orsay, IN2P3-CNRS, F-91405 Orsay Cedex, France

[c]Institut de Recherches Subatomiques (IReS), F-67037 Strasbourg, France

[d]Institute of Isotopes, H-1525 Budapest, Hungary

[e]KVI, University of Groningen, NL-9747 AA Groningen, Netherlands

[f]Institute of Nuclear Physics, N.C.S.R. Demokritos Athens, GR-15310 Athens, Greece

[g]Gesellschaft für Schwerionenforschung mbH (GSI), D-64291 Darmstadt, Germany

[h]Physikalisches Institut, Universität Tübingen, D-72067 Tübingen, Germany

The key reaction $^{12}C(\alpha,\gamma)^{16}O$ has been investigated in three different experiments at the Stuttgart DYNAMITRON in the course of international collaborations. In the energy range $E_{\mathrm{c.m.}} = 0.89 - 2.8\,\mathrm{MeV}$ He^+ beams of several hundred microamperes were directed on isotopically enriched carbon targets of high purity and with high beam power capabilities. To obtain γ angular distributions three different arrays of actively shielded HPGe detectors have been used to separate the $E1$ and $E2$ capture cross section which is necessary to describe and extrapolate the reaction in the energy range of stellar burning. The sensitivity of these experiments could be raised by a factor of 10–100 compared to previous investigations. The S-factor functions were fitted by an R-matrix analysis considering different data sets of α-capture, α elastic scattering and the decay of ^{16}N. The astrophysical reaction rate has been determined with $\pm 25\,\%$ accuracy in the temperature range $0.001 \leq T_9 \leq 10$.

The outstanding importance of the reaction $^{12}C(\alpha,\gamma)^{16}O$ is well known from literature [1]. Equally the complicated level structure of the daughter nucleus ^{16}O leading to nonpredictable interferences in the excitation functions of $E1$ and $E2$ capture has been discussed many times [2]. More than 30 experiments have been performed in the past three decades to determine the cross section, the extrapolated S-factor values S_{E1}^{300}, S_{E2}^{300}, and S_{tot}^{300} and the reaction rate. The published values and their uncertainties contradict

each other strongly: e.g. $S_{E1}^{300} = 1$–$288\,\mathrm{keVb}$, $S_{E2}^{300} = 7$–$120\,\mathrm{keVb}$, and $S_{\mathrm{tot}}^{300} = 40$–$430\,\mathrm{keVb}$ (see references in [3]). The reaction rate, determined from laboratory experiments, has been reported recently to have an uncertainty of $\pm 31\,\%$ [4], $\pm 41\,\%$ [5], $+85\,\% -57\,\%$ [6]. Several determinations of the $^{12}\mathrm{C}(\alpha,\gamma)^{16}\mathrm{O}$-reaction rate were deduced from astrophysical observations as for example the seismology of White Dwarfs [7] or from general nucleosynthesis models [8] as a consequence of the inconsistencies within the experimental data. At present an accuracy of $10\,\%$ is requested [9], stimulating new efforts for the experimental determination of this rate. Therefore two new experiments, characterized by high primary intensity ($0.5\,\mathrm{mA}$ He^+), a 4π-like detector setup, and sophisticated target technique have been undertaken to determine the $E1$ and $E2$ parts of the capture cross section in a wide energy range and thus to better constrain the astrophysical reaction rate. Two different 4π HPGe detector setups were constructed and optimized for the measurement of γ angular distributions: the special EUROGAM detector array shown in Fig. 1 and the GANDI array (**G**amma **AN**gular **DI**stribution Exp.), shown in Fig. 2.

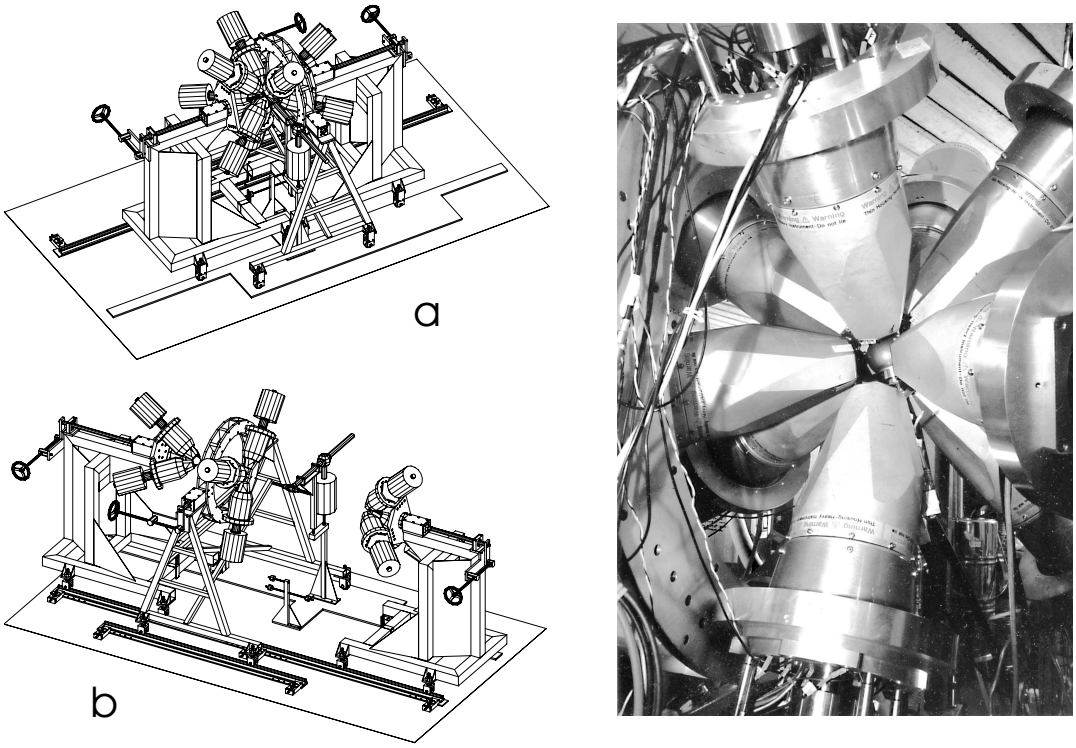

Figure 1. Left side: Sketch of the special 4π setup with 9 EUROGAM detectors. The upper part (a) shows the setup in the measuring configuration whereas the lower half (b) shows it in the service position with dispersed supports and easy access to target and detectors. Right side: Photo of the central part of the 4π detector setup in close geometry around the spherical target chamber at the center.

Special efforts were made to improve the quality of the targets during the production process and to determine their properties precisely. The $^{12}\mathrm{C}$ targets were enriched isotopically by magnetic separation and were implanted in or deposited on a gold backing of ultra high purity. The $^{13}\mathrm{C}$ depletion with respect to natural carbon was about 10^{-5}

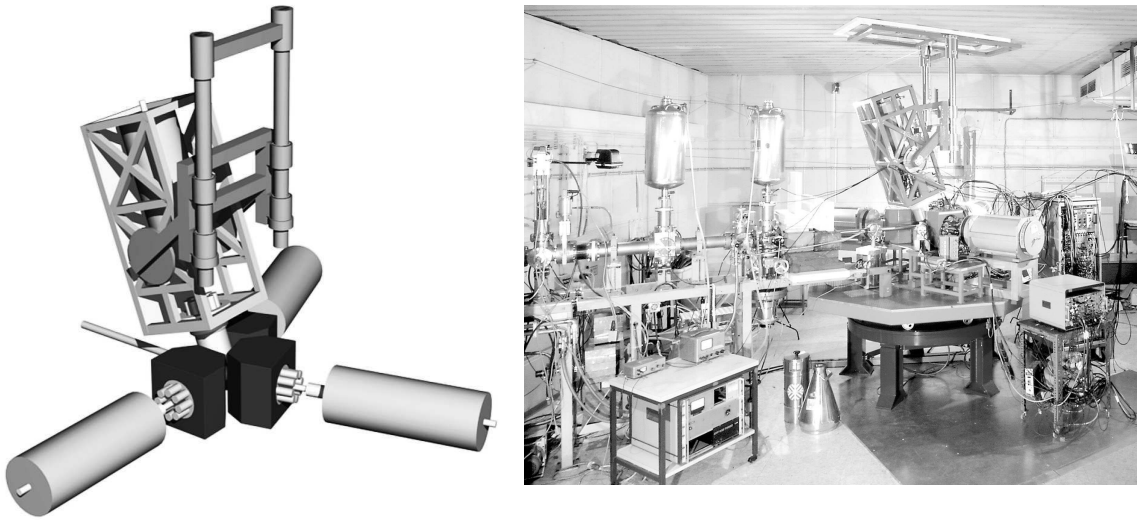

Figure 2. Sketch and photo of the GANDI detector array at the Stuttgart DYNAMITRON laboratory with four movable Ge (BGO) detectors in very close geometry. An angular distribution is obtained successively in three different positions of the lower three detectors.

bringing the $^{13}C/^{12}C$ ratio down to 10^{-7} with respect to the separation. But the real $^{13}C/^{12}C$ ratio was limited to 10^{-5} by a small, unavoidable carbon content in the gold layer, which was determined by (α,n)-measurements. The implantation energies were 70 keV and 20 keV at implanters in Bochum and Orsay (SIDONIE) respectively, with target densities ranging from 1–11 $\times$ 10^{18} atoms/cm^2. A series of targets with improved design, shown in Fig. 3 (left side), were deposited with energies of up to 1 keV and densities of 2×10^{18} atoms/cm^2. The deposition technique yields a more stable surface layer with a diamond-like ^{12}C structure, better stoichiometry, and about twice the beam survival time of implanted targets. The target depth profile and areal distribution were measured precisely using the ARAMIS accelerator RBS facility at Orsay. Based on these measurements the spatial ^{12}C distributions, which are necessary to determine the target density and the effective beam energy, were determined before and after the bombardment with $^4He^+$ beam. Fig. 3 (right side) shows a typical example of a target profile after irradiation with 90.6 C of $^4He^+$. The average target degradation due to the bombardment was less than 20 %. Special care has been taken to maintain ultraclean conditions in the beam line such as a vacuum of a few times 10^{-8} mbar, and the surveillance of the neutron background by a sensitive NE213 neutron spectrometer.

With the 4π EUROGAM array a total of 25 γ angular distributions were measured. For each distribution a beam charge of typically 10–30 C was collected. Details with figures and tables are given in [10]. In the second experiment using the GANDI array 12 γ angular distributions were measured in the low energy range with 500 μA $^4He^+$ beam current. For the lowest point, at $E_{\mathrm{c.m.}} = 891$ keV, a beam charge of 164 C was collected, yielding a cross section in the range of a few picobarns. The results of the GANDI experiment are given in detail in [3] and in short form in [23]. The γ spectra were analyzed by using experimentally determined line shapes for the least square fitting of weak γ lines. The

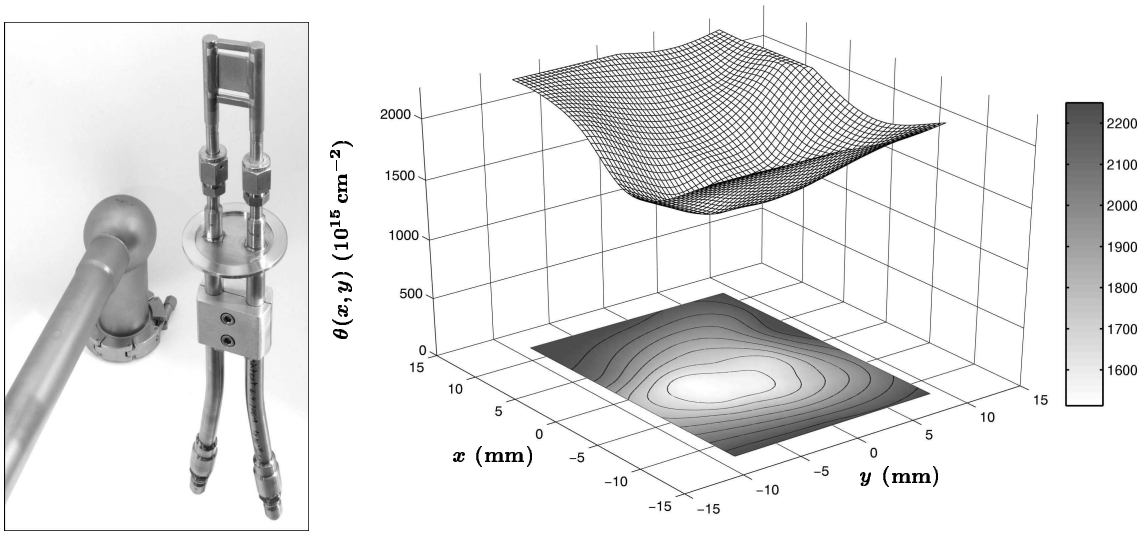

Figure 3. Left side: Photo of the high beam power target designed for 10 kW/cm^2. The backing consists of a 2mm thick copper plate with 14 cooling channels. The water pressure is typically 50 bar and the flow velocity about 25 m/s, the water connections inside the vacuum are metal sealed. On the gold plated backing ^{12}C is mass separated and deposited with about 2×10^{18} atoms/cm^2. Right side: Density profile θ of a ^{12}C target after irradiation with 90.6 C ^{4}He$^+$. This profile was obtained by RBS scanning of the target surface.

effects of finite geometry have been corrected, in part by applying GEANT simulations.

The values for σ_{E1} and σ_{E2} have been obtained from the γ angular distributions by using the formula for the interference of $E1$ and $E2$ transitions in angular distributions, given in the paper of Dyer and Barnes [11]. The parameter ϕ_{12} (phase) of this formula was not kept open, but determined by using the elastic α-scattering data of Plaga *et al.* [12] and D'Agostino Bruno *et al.* [13] and indirectly also of Tischauser *et al.* [14] to avoid insufficient separation and subsequent transfer of $E1$ yield to the $E2$ channel around the 1^- resonance. This treatment has already been proposed by Barker [15].

The R-matrix calculations were performed using the code ERMA of Kunz [4,16]. They are based on the Stuttgart capture data for $E1$ and $E2$ (EUROGAM, GANDI, Kunz *et al.*), the scattering phases of [12,13], and the data of the β-delayed α-decay of ^{16}N [17]. There are three reasons to use only the three most recent data sets: a. these data have been evaluated in a consistent manner concerning all corrections and the treatment of uncertainties; b. 57 data points are sufficient for the R-matrix fits at the present level of accuracy; c. for data of other experiments a re-evaluation of the uncertainties would be necessary. The $E1$-excitation function has been described by a three-level-R-matrix fit ($E_R = -45.1$ and 2400 keV + 'background'-level) assuming a radius $R_0 = 6.5$ fm for the inner space with the nuclear interaction which was also used by Barker and Kajino [18] and Angulo and Descouvemont [19]. The R-matrix fit for $E1$ is shown in Fig. 5 in 4 graphs, giving the result for the four possible interference sign combinations (a – d). The boundary parameter was chosen in a way to obtain physically relevant parameters for the

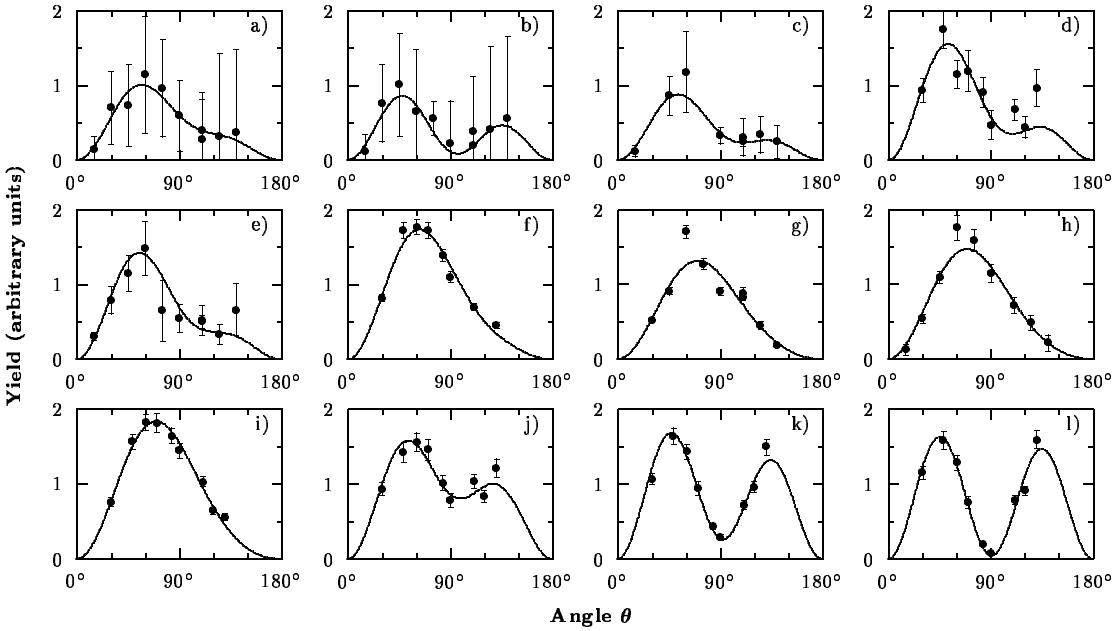

Figure 4. Typical γ angular distributions measured at the following effective c.m. energies: a) 891 keV, b) 903 keV, c) 1102 keV, d) 1342 keV, e) 1452 keV, f) 1965 keV, g) 2209 keV, h) 2221 keV, i) 2267 keV, j) 2645 keV, k) 2660 keV, l) 2667 keV. The solid curves represent the relevant Legendre fits. The error bars shown here include also systematic uncertainties. The $E1$, $E2$ characteristics and interferent mixing of both can be seen clearly. From these angular distributions σ_{E1} and σ_{E2} were separated and deduced.

subthreshold levels; so γ-widths and energies from literature [22] could be used. A five-level-fit could not improve the description of S_{E1} because of the lack of data at energies above 4 MeV. The $E2$-data have been described with a five-level-R-matrix fit (-245, 2680, 4320, 5650 keV and the 'background'-level) using again the elastic scattering data from literature for $l=2$ [12,13], γ-widths [22] and the resonance parameters for the 2^+ resonance [22]. This fit is consistent with the more recent elastic scattering data of Tischhauser *et al.* [14]. Using a five-level-R-matrix fit yields in total 16 interference sign combinations and a sufficient number of parameters to describe all details of the experimental and the literature data. In Fig. 6 the graphs of four sign combinations out of 16 and the obtained excitation functions are shown (A – D). The fit of graph D with the lowest χ^2 was taken to calculate the reaction rate.

In order to obtain a better assessment of the relevance of the different capture data sets, the R-matrix calculations were carried out for six cases: the EUROGAM (A) and the GANDI (B) experiment alone, and additionally the 20 data points (C) of Kunz *et al.* [16] were included; further for the combinations of data sets (A + B), (B + C), and (A + B + C). Table 1 shows the 300 keV extrapolated values for the different data sets and their combinations. The agreement between the fits is very good, the combination of the three data sets from the recent DYNAMITRON experiments (A+B+C) gives the lowest uncertainty and is our final result [3,23].

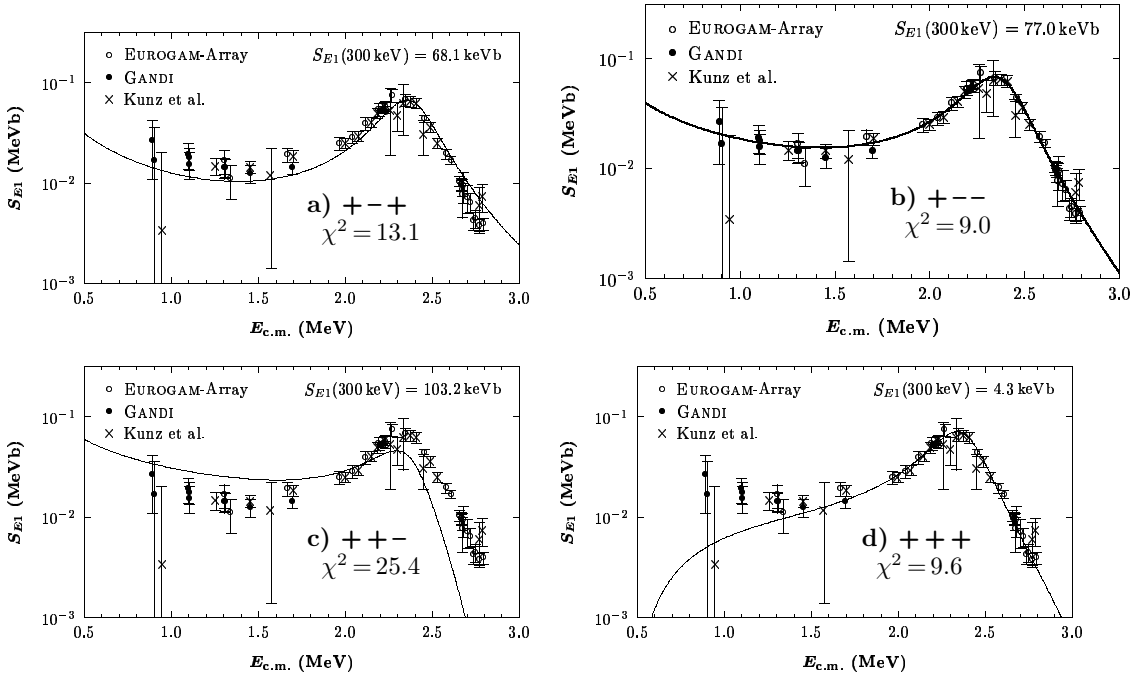

Figure 5. S-factors for $E1$ capture in $^{12}\mathrm{C}(\alpha,\gamma)^{16}\mathrm{O}$. The experimental data are taken from the EUROGAM [10] and the GANDI experiment [3,23] and from Kunz *et al.* [16]. The solid curves in diagram a – d represent the three-level-R-matrix fit to the data with four possible interference combinations. The sign combination $+--$ (diagram b) yields the best fit to the experimental data with the smallest χ^2. This combination was used for the calculation of the reaction rate. Not shown here is the simultaneous fit to the α-spectrum of the ^{16}N-decay [17] and to the data of elastic α-scattering from ^{12}C [12,13],([14]). The extrapolation values of the S-factors at 300 keV are given in Tab. 1.

The capture data of the present experiments (EUROGAM, GANDI) cover the energy range $E_{\mathrm{c.m.}} = 0.89 - 2.8\,\mathrm{MeV}$. Because of the lack of experimental data at higher energies the resonance parameters for the R-matrix description have been taken from Tilley *et al.* [22]. The S-factor for contributions by cascade transitions $S^{300}_{casc} = 4\,(4)\,\mathrm{keVb}$ has been taken from Kunz *et al.* [16]. The contributions of resonances with other multipolarities were calculated using data from Tilley *et al.* [22] and assuming Breit-Wigner curves with energy dependent widths but without making assumptions on their unknown interference terms.

Table 1
Extrapolation values S^{300}_{E1} and S^{300}_{E2} for the different combination of data sets A, B, and C (A = EUROGAM, B = GANDI, C = Kunz *et al.*). For all cases also data of elastic scattering [12–14] and ^{16}N decay [20,21] were considered. The result of case A + B + C yields the lowest uncertainty and is used for the calculation of the reaction rate.

Data from :	A	B	C	A + B	B + C	A + B + C
S^{300}_{E1} (keV b)	81 (20)	77 (19)	76 (20)	77 (19)	76 (18)	77 (17)
S^{300}_{E2} (keV b)	80 (27)	78 (26)	85 (30)	80 (25)	81 (23)	81 (22)
S^{300}_{tot} (keV b)	—	—	165 (50)	—	—	162 (39)

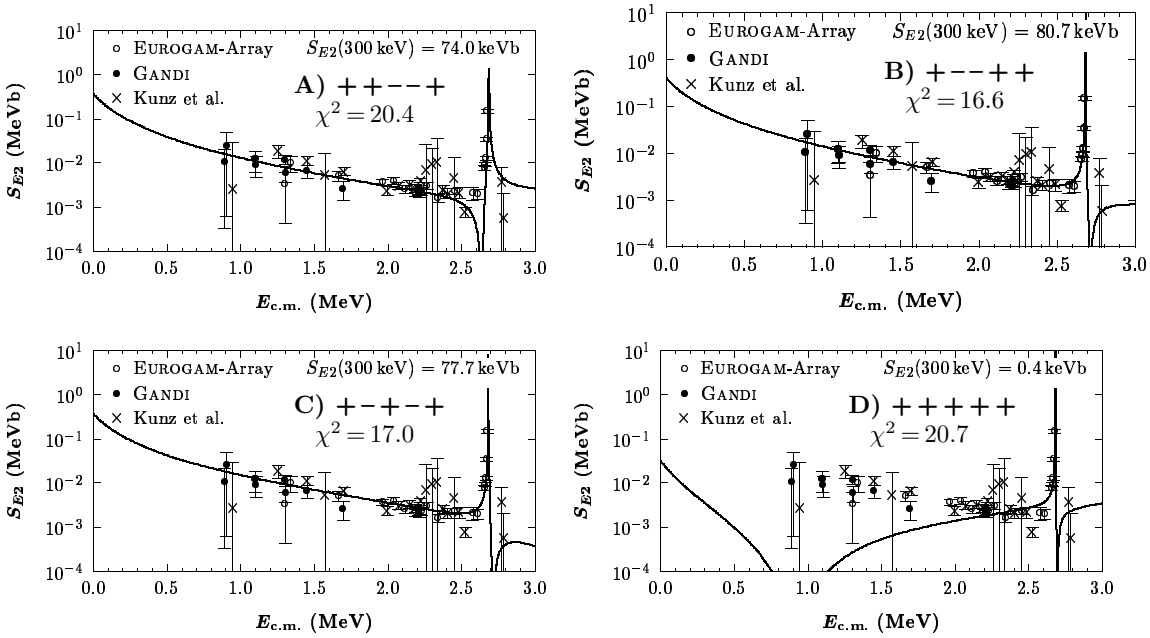

Figure 6. S-factors for $E2$ capture in $^{12}\mathrm{C}(\alpha,\gamma)^{16}\mathrm{O}$ from 3 experiments (EUROGAM [10], GANDI [3,23] and Kunz *et al.* [16]) and from a five-level-R-matrix fit (solid lines). In the fit also a fit to α-elastic scattering data was included [12,13],([14]). When using a five-level-R-matrix analysis one obtains 16 possible interference sign combinations, four of them are shown in graph A – D. The best fit ($\chi^2 = 16.6$) was obtained for the sign combination $+--++$ and it was used for the calculation of the reaction rate. Most of the other sign combinations can now be ruled out because the fit deviates from the experimental data.

The astrophysical reaction rate was obtained by the convolution of the excitation functions (Figs. 5,6) with corresponding Maxwell-Boltzmann distributions of α-particles by numerical integration. This new rate has a maximum total uncertainty of $\pm 25\,\%$. For the reaction rate the usual analytical form has been given by the following equations [6,4]:

$$N_A\langle\sigma v\rangle = r_1 + r_2 + r_3 + r_4 \qquad [\mathrm{cm}^3(\mathrm{s}\cdot\mathrm{mol})^{-1}]$$

$$r_1 = \frac{a_0}{T_9^2\left(1 + a_1\,T_9^{-2/3}\right)^2}\,\exp\left(-\frac{a_2}{T_9^{1/3}} - \left(\frac{T_9}{a_3}\right)^2\right) \qquad r_2 = \frac{a_4}{T_9^2\left(1 + a_5\,T_9^{-2/3}\right)^2}\,\exp\left(-\frac{a_6}{T_9^{1/3}}\right)$$

$$r_3 = \frac{a_7}{T_9^{3/2}}\,\exp\left(-\frac{a_8}{T_9}\right) \qquad r_4 = \frac{a_9}{T_9^{2/3}}\left(1 + a_{10}\,T_9^{1/3}\right)\exp\left(-\frac{a_{11}}{T_9^{1/3}}\right).$$

The fit parameters for the analytical expression of the $^{12}\mathrm{C}(\alpha,\gamma)^{16}\mathrm{O}$ reaction rate are:

$a_0 = 1.51\times10^8$; $a_1 = 0.0666$; $a_2 = 32.12$; $a_3 = 1.03$; $a_4 = 1.11\times10^9$; $a_5 = 0.735$; $a_6 = 32.12$; $a_7 = 0.0$; $a_8 = 0.0$; $a_9 = 16200$; $a_{10} = 2.19\times10^6$; $a_{11} = 38.814$.

The analytical expression is valid in the full temperature range of $0.001 \le T_9 \le 10$ reproducing the reaction rate with a maximum uncertainty of $8\,\%$. In the most interesting

temperature range of $T_9 = 0.1 - 0.3$ this uncertainty is only 1 %.

At burning temperature $T_9 = 0.2$ this new reaction rate is about 8 % higher than the rate given by Buchmann [6], about 20 % lower than the rate given by the NACRE collaboration [5], and it agrees well with the rate of Kunz *et al.* [4]. The temperature dependence of this rate differs from those of Buchmann and NACRE, especially at higher temperatures.

Summing up, we have measured 37 new γ angular distributions each consisting of 8–10 data points to deduce new reaction rates for $^{12}C(\alpha,\gamma)^{16}O$. It is worth mentioning that the angular distribution at the lowest energy (891 keV) has been measured with the highest sensitivity reached by any experiment of this kind. From the angular distributions the excitation functions of $E1$ and $E2$ captures were successfully separated. We claim that our results put strong constraints on the reaction rate since the data of three independent experiments are in very good agreement (see Table II) and contribute to the final result. Several works on stellar models are still based on older reaction rates [24,25] which are superseded by this result. Variations of the reaction rate by a factor of two or even higher found in other experiments are not consistent with our experimental findings. It should be pointed out that experiments with a much lower sensitivity (factor 100) have claimed about the same uncertainties; therefore results should be compared with great care.

REFERENCES

1. T. Rauscher et al., Astrophys. J. 576 (2002) 323.
2. K. Langanke and C.A. Barnes, in: Adv. in Nucl. Phys. **22**, Eds. J.W. Negele and E. Vogt (New York, 1996), p. 173–263
3. M. Fey, PhD thesis, Stuttgart, Germany (2004), http://elib.uni-stuttgart.de/opus/volltexte/2004/1683/
4. R. Kunz et al., Astrophys. J. 567 (2002) 643.
5. C. Angulo et al., ("NACRE"), Nucl. Phys. A 656 (1999) 3.
6. L. Buchmann, ApJL. 468 (1996) L 127.
7. T.S. Metcalfe, D.E. Winget, P. Charbonneau, ApJ **557** (2001) 1021.
8. T.A. Weaver and S.E. Woosley, Phys. Rep. **227** (1993) 65.
9. S.E. Woosley et al., Nucl. Phys. A718 (2003) 3c.
10. M. Assunção et al., submitted to Phys. Rev. C (2004).
11. P. Dyer and C.A. Barnes, Nucl. Phys. **A 233** (1974) 495.
12. R. Plaga et al., Nucl. Phys. A 465 (1987) 291.
13. M. D'Agostino Bruno et al., Nuovo Cimento Soc. Ital. Fis. 27 (1975) 1.
14. P. Tischhauser et al., Phys. Rev. Lett. 88 (2002) 072501.
15. F.C. Barker, Aust. J. Phys. **24** (1971) 777.
16. R. Kunz et al., Phys. Rev. Lett. 86 (2001) 3244.
17. R.E. Azuma *et al.*, Phys. Rev. C **50** (1994) 1194.
18. F.C. Barker and T. Kajino, Aust. J. Phys. **44** (1991) 369.
19. C. Angulo and P. Descouvemont, Phys. Rev. C **61** (2000) 064611.
20. L. Buchmann et al., Phys. Rev. Lett. 70 (1993) 726.
21. L. Buchmann et al., Phys. Rev. C 54 (1996) 393.
22. D.R. Tilley et al., Nucl. Phys. A 564 (1993) 1.
23. M. Fey et al., submitted to Phys. Rev. (2004).
24. G.R. Caughlan et al., ("CFHZ85"), At. Data Nucl. Data Tables 32 (1985) 197.
25. G.R. Caughlan and W.A. Fowler, ("CF88"), At. Data Nucl. Data Tables 40 (1988) 283.